Geochemical Perspectives Letters



# Textural and chemical inheritance during a pseudomorphic double mineral transformation

P. Forjanes[1*], J.P.H. Perez[1], C. Berryman[1], M. Syczewski[1,2], L.G. Benning[1,3]

OPEN ACCESS

https://doi.org/10.7185/geochemlet.2513

## Abstract

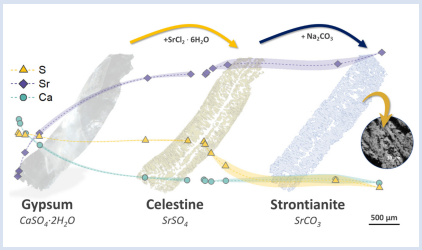


Pseudomorphism, a prominent feature of many fluid-driven mineral transformations, happens when a secondary phase inherits the morphology of the primary one due to a tight coupling between primary phase dissolution and secondary phase precipitation. Pseudomorphic transformations are common in nature, yet the fate of pseudomorphs, once formed, has been largely overlooked. Here, we assess the double pseudomorphic transformation of i) gypsum ($CaSO_4{\cdot}2H_2O$) to celestine ($SrSO_4$), and ii) of the so-formed celestine to strontianite ($SrCO_3$). Through detailed mineralogical and geochemical analyses we document two successive pseudomorphic mineral replacement transformations. Both replacements occur through a coupled mechanism of dissolution-crystallisation, are complete, fast, and occur while preserving the external morphology of the gypsum precursor. The two transformations lead to the development of two generations of pores within the replaced phase(s), caused by the decrease in molar volume associated with both transformations. Interestingly, the final strontianite pseudomorphs inherit not just the texture but also chemical features of both the gypsum precursor and the intermediate celestine. Our findings highlight the ability of pseudomorphs to record and preserve chemical and textural information in successive transformations, underlying their relevance as resilient geological proxies.

Received 14 October 2024 | Accepted 23 March 2025 | Published 17 April 2025

## Introduction

Minerals undergo phase transformation reactions in response to changing environmental conditions (Putnis, 2002, 2009; Ruiz-Agudo *et al.*, 2014). At Earth (sub)surface conditions, these mineral transformations are usually driven by fluids. Typically, such fluid-driven reactions proceed through the dissolution of a primary phase and the subsequent precipitation of a secondary one. These two steps are often coupled in space and time, often resulting in pseudomorphic mineral products (Putnis, 2002, 2009). The degree of coupling between dissolution and crystallisation determines the fidelity with which the secondary phase replicates the micro- and nano-textural features of the parent mineral phase (Xia *et al.*, 2009). Unsurprisingly, pseudomorphism has been a subject of scientific interest for over two centuries as pseudomorphs constitute crucial geological proxies recording fluid-driven mineral processes in sedimentary (Leitner *et al.*, 2013), igneous (Nozaka and Fryer, 2011) and metamorphic settings (Centrella *et al.*, 2015).

Once the dissolving primary phase is fully carpeted by crystals of the precipitating secondary phase, the replacement typically progresses inwards through the formation of a network of pores. Porosity arises from the difference in molar volume and solubility between the initial and final phases. Furthermore, this porosity plays a key role in allowing the reaction to proceed from the outside to the inside, facilitating fluids to penetrate towards the reaction front (Putnis, 2002, 2009; Ruiz-Agudo *et al.*, 2014; Altree-Williams *et al.*, 2015). Even though many pseudomorphic mineral replacement reaction systems have been studied over the last decades, the long term fate of such pseudomorphs has barely received attention. The porosity formed during these transformations usually has a transient nature and tends to reorganise and close (Jonas *et al.*, 2014; Putnis, 2015; Beaudoin *et al.*, 2018). Additionally, the consequences of the interaction between freshly formed pseudomorphs and new solutions of different composition, is unknown. This is striking, considering that numerous naturally occurring pseudomorphs, which host different mineral phases, have been reported in nature (Dempster and Jess, 2015). Addressing this latter issue is the aim of this study. Here, we seek to understand how a double pseudomorphic replacement operates, and if any textural and/or chemical features useful to trace the history of the pseudomorphs are preserved during the successive transformations. To do so, we have studied the transformation of gypsum ($CaSO_4{\cdot}2H_2O$) into celestine ($SrSO_4$), followed by their subsequent transformation into strontianite ($SrCO_3$). Individually, both replacement reactions proceed rapidly (gypsum-celestine, Forjanes *et al.*, 2020a; and celestine-strontianite, Pina *et al.*, 2019) and are therefore an ideal model system. Yet, the parameters controlling the evolution of the mineralogy, chemical composition and texture (*i.e.* porosity, organisation of secondary crystals, *etc.*) of a pseudomorph when it itself undergoes a second transformation are unknown.

[1] GFZ Helmholtz Centre for Geosciences, 14473, Potsdam, Germany
[2] University of Warsaw, Faculty of Biology, 02-096, Warsaw, Poland
[3] Department of Earth Sciences, Freie Universität Berlin, 12249, Berlin, Germany
* Corresponding author (email: pablo.forjanes@gfz.de)

## Materials and Methods

We followed the consecutive conversion: (i) of gypsum single crystals to celestine, and (ii) of the so-formed celestine to strontianite. Small gypsum single crystals (Teruel, Spain) were first reacted with 1 mL of a 0.5 M Sr-bearing solution, leading to their complete replacement by celestine within one day. Following this, half of the so-formed celestine crystals were reacted with 1 mL of a 0.5 M carbonate-rich solution to transform them into strontianite. Initial, intermediate, and end products of the interacted materials were analysed using powder X-ray diffraction (pXRD), Fourier transform infrared (FTIR) spectroscopy, and scanning electron microscopy (SEM). The porosity development, indicated by changes in surface area, was followed with nitrogen gas sorption analysis using the Brunauer-Emmett-Teller (BET) model. Finally, the changes in chemical composition of the crystals and of the reacting solutions were determined *via* inductively coupled plasma optical emission spectrometry (ICP-OES). For detailed information on all experimental procedures and characterisation methods see Supplementary Information.

## Results and Discussion

***The transformation of gypsum ($CaSO_4{\cdot}2H_2O$) single crystals into celestine ($SrSO_4$).*** The interaction between gypsum and the Sr-rich solutions results in their full replacement by celestine within one day, as evidenced by pXRD, FTIR and ICP-OES data (Figs. 1a,b, S-3 and S-4, Table S-3). The replacement takes place through a dissolution-crystallisation mechanism and begins as soon as the gypsum crystal comes into contact with the Sr-rich solution. Our solution data reveal that gypsum immediately starts to dissolve, releasing calcium and sulfate ions into the solution (Table S-3). The dissolution of gypsum should hypothetically continue until the solution reaches equilibrium with respect to this mineral ($K_{sp} = 10^{-4.58}$; PHREEQC database). However, before this occurs, the fluid becomes saturated with respect to celestine ($K_{sp} = 10^{-6.63}$, SI 3.03; Howell *et al.*, 1992), causing this mineral to precipitate on the surfaces of the gypsum parent material, as observed in our results (Fig. 1c). The precipitation of celestine depletes the sulfate released during the dissolution of gypsum, triggering further dissolution of the later mineral. This establishes a gypsum dissolution–celestine crystallisation loop, which operates until the complete replacement of the parent crystal is achieved. This interpretation is supported by the evolution of the ion concentrations in the solution (Fig. S-5) that reveal that, upon reacting gypsum (~150 mg) with ~15 mL of the Sr-bearing solution, the interacted fluid now contains ~54 mM of $Ca^{2+}$, corresponding to a release of ~99 % of the Ca present in the precursor (Table S-3, Fig. S-5). Surprisingly, dissolved sulfate concentrations remain low (<1 mM) throughout the experiments, suggesting that all the sulfate released during gypsum dissolution is rapidly captured to precipitate celestine. The external morphology of the parent gypsum is preserved, resulting in celestine pseudomorphs after gypsum. (Fig. S-6). In fact, this pseudomorphism is so perfect that even µm-scale features of the original gypsum surface (*e.g.*, exfoliation steps) are preserved during its conversion into celestine. Xia *et al.* (2009) defined the concept of length-scale of pseudomorphism, stating that for a fluid-driven mineral transformation to achieve perfect pseudomorphism, dissolution and precipitation have to be strongly coupled. This condition is typically met when the transformation kinetics are controlled by the dissolution of the primary mineral. Our SEM observations, which evidence pseudomorphism occurring even at the micro-scale, point to this scenario. This is consistent with the results of ICP-OES data showing a permanently low concentration of sulfate in the fluid. The early celestine crystals growing on the gypsum surfaces exhibit distinct prismatic habits with flat and well developed faces (Fig. 1c). Their growth is initially concentrated near the exfoliation steps of the gypsum surfaces, which are the most reactive areas (Fig. S-7). However, with time, the majority of the crystals exhibit sheaf-like and spherulitic morphologies (Fig. 1d). Such a morphological evolution is related to the incorporation of Ca coming from gypsum dissolution into the crystal structure of the growing celestine, where it replaces Sr (Forjanes *et al.*, 2020a, 2020b), an observation supported by EDS and ICP-OES analyses on the solids (Table S-3, Fig. 1b). This morphological evolution of minerals due to incorporation of other ions into their structures is a well documented phenomenon in the literature (Fernández-Díaz *et al.*, 2006; Shtukenberg *et al.*, 2012).

The pseudomorphic replacement of gypsum by celestine involves a significant difference in molar volume between primary gypsum, (74.31 $cm^3$/mol) and secondary celestine (46.25 $cm^3$/mol). When gypsum is transformed pseudomorphically into celestine, in order to compensate for this volume decrease, a considerable volume of porosity is generated within the newly formed phase (Fig. 1e,f), accompanied by an increase in the BET surface area (<0.01 $m^2$/g in gypsum *vs.* 0.54 $m^2$/g in celestine; Fig. S-8). This porosity plays a key role in facilitating the rapid progression of the transformation, as it allows the solution to reach the reaction front, enabling the replacement reaction to proceed easily (Fig. 1e,f). Based on the evaluation of SEM images of polished sections, we determined the 2D porosity reduction to be 38 %, a value close to the theoretical reduction in molar volume between gypsum and celestine (−37.76 %). The newly formed pore network is arranged in channels perpendicular to the gypsum surfaces, and distributed between elongated celestine crystals. This stockade-like distribution of the celestine aggregates and the associated porosity can be attributed to the competitive growth between celestine crystals during the transformation. All celestine crystals in the replaced layer appear with their *c* axis perpendicular to the gypsum surface, as only crystals growing in this direction can grow without interference. In contrast, crystals oriented differently cannot grow due to the lack of available pore space. A similar phenomenon has been observed in other fluid-driven mineral replacement systems (Pöml *et al.*, 2007; Fernández-Díaz *et al.*, 2009; Zhao *et al.*, 2009).

***The second pseudomorphic transformation: celestine ($SrSO_4$) to strontianite ($SrCO_3$).*** In the second transformation, the interaction between the celestine pseudomorphs and a carbonate-rich solution leads to a second replacement of the pseudomorphs by strontianite. This also occurs through a dissolution-precipitation reaction and happens within one day, as confirmed by pXRD, ICP-OES and FTIR data (Figs. 2a,b, S-4 and S-9, Table S-3). The most interesting feature is that this second replacement reaction is also pseudomorphic, and occurs while (again) preserving the external morphology of the original gypsum precursor. Thus, this second replacement results in the formation of strontianite pseudomorphs after gypsum, produced *via* intermediate celestine (Fig. S-10). This transformation again proceeds *via* a coupled mechanism of celestine dissolution and strontianite precipitation ($K_{sp} = 10^{-9.27}$, SI 1.94; De Villiers, 1971). ICP-OES analysis of the reacted fluids show that ~99 % of the total S from celestine is released into the fluid during the transformation, while the aqueous Sr concentrations remain low throughout the whole reaction (Table S-4 and Fig. S-11), indicating that all the Sr released during the dissolution of celestine is rapidly captured to form strontianite.

SEM images of the surfaces of the reacted celestine pseudomorphs after 10 min of reaction with the carbonate-rich solution reveal that each celestine crystal is, in turn,

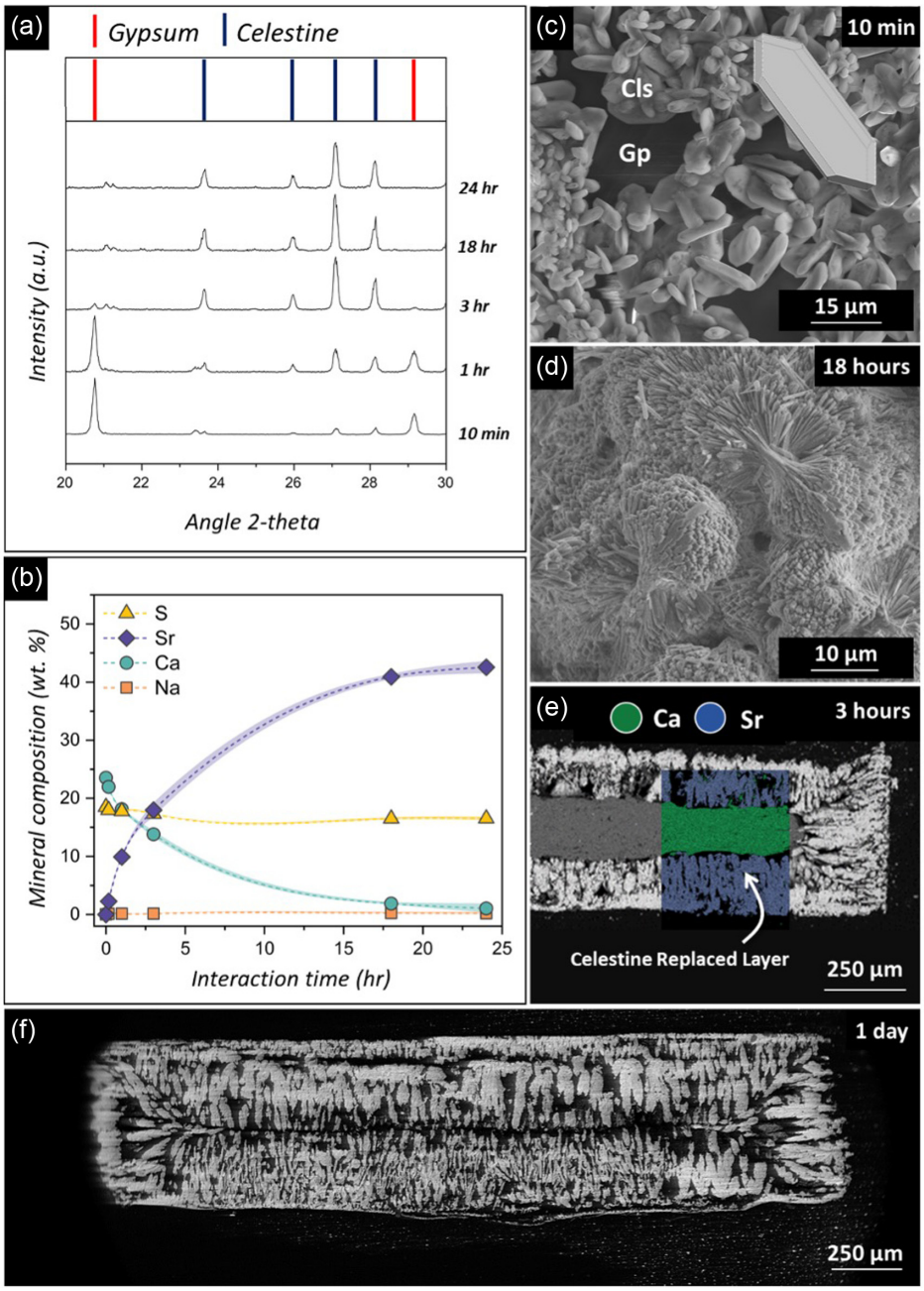


**Figure 1** **(a)** Selected pXRD data showing the full replacement of gypsum single crystals (Gp; red lines) by celestine (Cls; blue lines). **(b)** Composition of the digested solids after increasing reaction times derived from ICP-OES data. **(c, d)** Prismatic celestine crystals initially grow on gypsum surfaces, and as the reaction progresses, spherulitic habits become dominant. **(e, f)** The interaction results in the full pseudomorphic replacement of gypsum by celestine. Images **(c–f)** were obtained in the SEM using SE **(c, d)** and BSE **(e, f)**.

pseudomorphically replaced itself by tiny crystals of strontianite (<0.5 µm) (Fig. 2c,d) initially growing on the surfaces of the celestine ones (Fig. 2e). Nevertheless, in each pseudomorphically replaced celestine crystal, the morphology of the celestine precursor remains perfectly preserved (Fig. 2d) and even the celestine spherulites appear pseudomorphically replaced by strontianite (Fig. 2f). The preservation of the external morphology of the initial gypsum precursor is possible because every individual celestine crystal that formed in the first pseudomorphic transformation is itself pseudomorphically transformed into strontianite in the 2nd reaction. Consequently, the final outcome of the two mineral replacements are pseudomorphs of strontianite after gypsum comprised of thousands of pseudomorphs of strontianite after the intermediate celestine. The ICP-OES analyses of the digested strontianite crystals evidence that they inherit not only textural features of the two previous phases, but also part of the chemical information. Despite being compositionally and mineralogically a totally new phase, the final strontianite ($SrCO_3$) pseudomorphs still contain trace amounts of both Ca (~0.59 wt. %), from the gypsum precursor, and S (~0.51 wt. %), from the intermediate celestine (Table S-3).

The textural preservation after the second pseudomorphic transformation, documented through SEM images of polished sections (Fig. 3), reveals that the replaced crystals still display the texture developed during the first gypsum to celestine replacement reaction: long aggregates perpendicular to the gypsum original surfaces with channel-arranged pores in between them. This texture is perfectly preserved, without evidence of pore infilling,

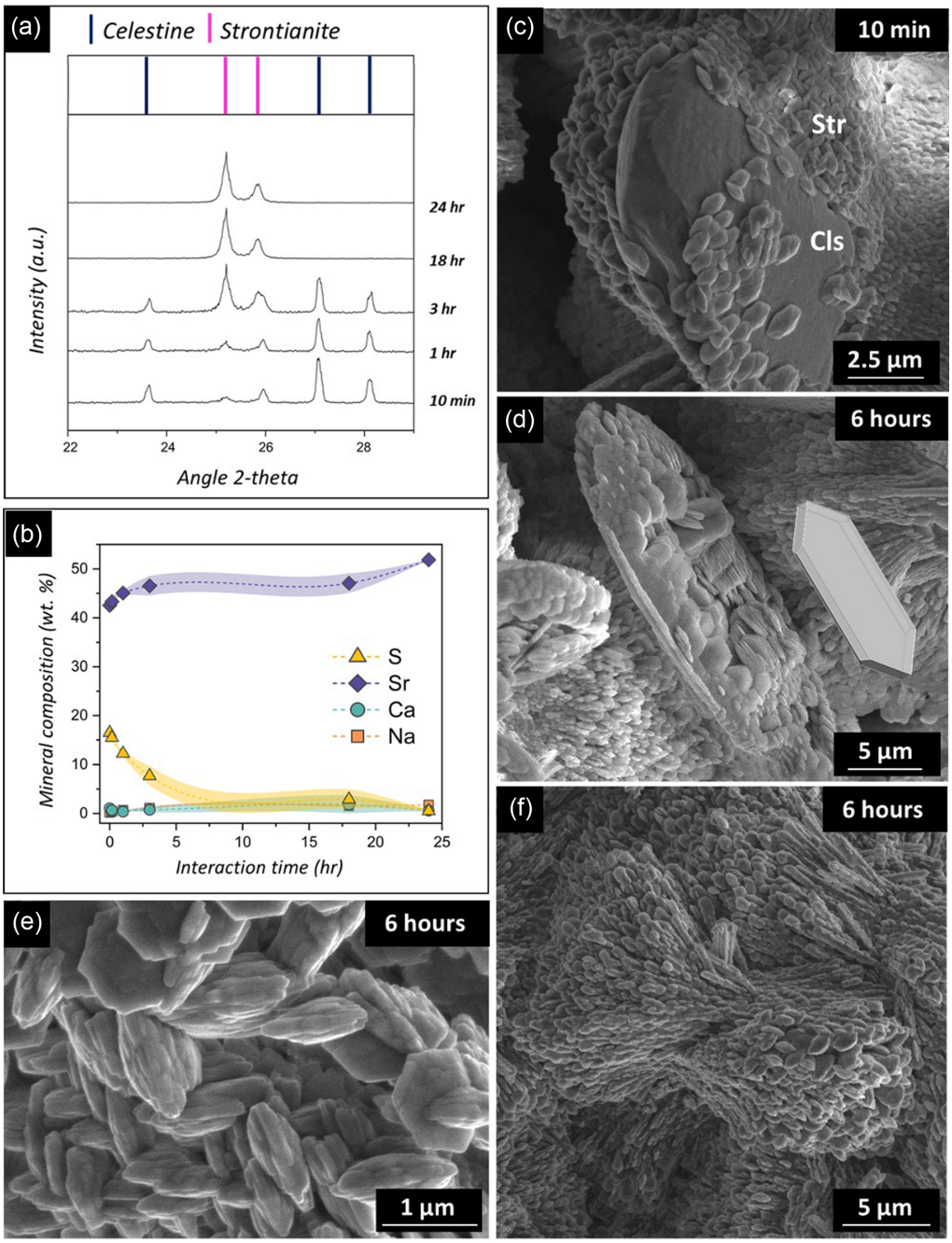


**Figure 2** **(a)** Selected pXRD data showing the full replacement of the celestine pseudomorphs (Cls; blue lines) by strontianite (Str; pink lines). **(b)** Composition of the digested solids derived from ICP-OES data. **(c–e)** During the transformation, each celestine crystal that makes up the first pseudomorph is itself pseudomorphically replaced by tiny crystals of strontianite with the characteristic pseudohexagonal morphology of the aragonite group minerals (Deer *et al.*, 2013). **(f)** Celestine spherulites are also pseudomorphically replaced by strontianite. Images **(a–f)** were obtained in the SEM using SE.

during the second transformation of the aggregates into strontianite (Fig. 3a). However, the second transformation of celestine (46.25 $cm^3$/mol) to strontianite (39.01 $cm^3$/mol) also involves a decrease in molar volume (−15.6 %) which is, once again, compensated by the generation of additional porosity. This additional porosity forms within each transformed celestine crystal (Fig. 3b; 13.5 % according to measurements made on SEM images). After the two consecutive mineral transformations, this produces two generations of pores: (i) a first generation of channel-arranged pores formed during the first gypsum to celestine transformation that are dispersed in between the elongated celestine aggregates, and (ii) a second generation of pores formed during the transformation of celestine into strontianite that forms within each of the transformed celestine aggregates. This second transformation and pore generation also increased the BET specific surface area, from 0.54 $m^2$/g in the celestine pseudomorphs to 3.75 $m^2$/g in the strontianite ones (Fig. S-8).

The progression of the second mineral transformation is documented in the polished sections of celestine pseudomorphs only partially replaced by strontianite after 3 hr of reaction, where each celestine aggregate is surrounded by porous rims of strontianite (Fig. 3c–e). This indicates that, similar to the gypsum crystal replacement by celestine, the replacement of each celestine aggregate by strontianite also occurs from the outside to the inside due to the penetration of the carbonate-rich solution through the newly formed second generation porosity.

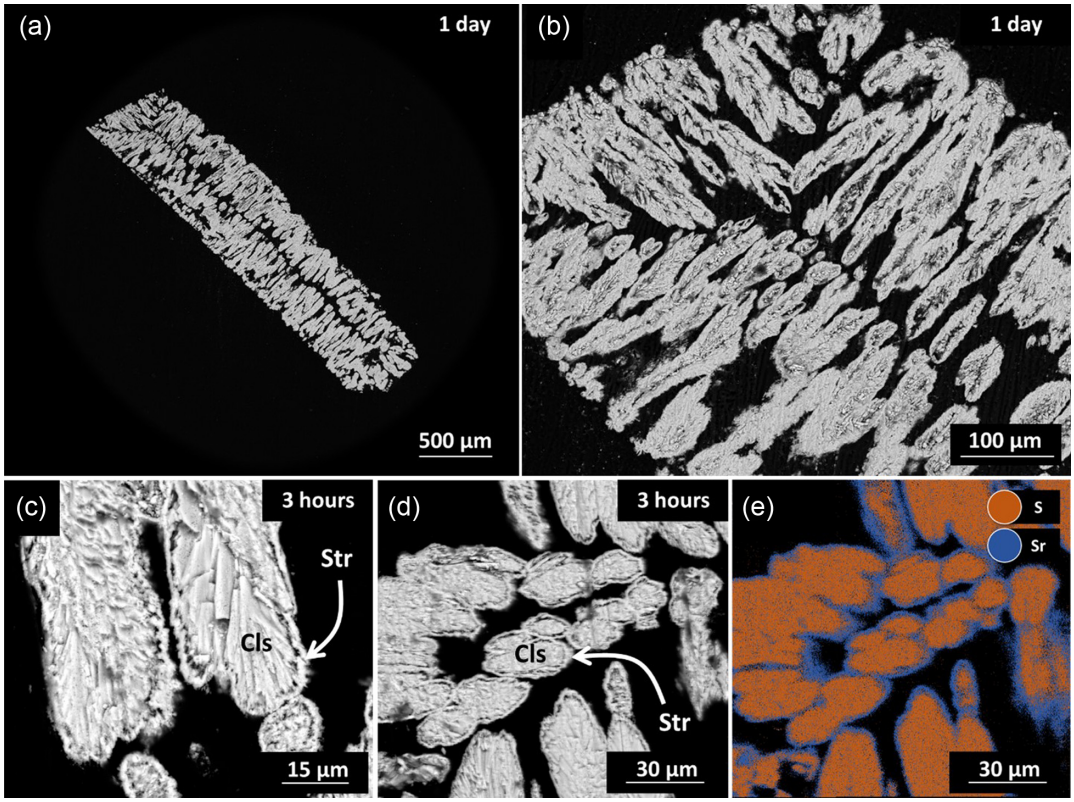


**Figure 3** Polished sections of celestine pseudomorphs obtained in the SEM using BSE after **(a, b)** 1 day and **(c–e)** 3 hr interaction with a $Na_2CO_3$ solution. **(a, b)** The replacement of the celestine pseudomorphs by strontianite preserved the texture developed in the previous transformation. **(c–e)** Images of partially replaced pseudomorphs after 3 hr of reaction.

After the first transformation of gypsum into celestine, the celestine aggregates, exhibited a compact appearance and a homogeneous surface (Fig. 4a). However, this changes significantly after the second transformation of celestine into strontianite (Fig. 4), where these transformed aggregates host a considerable additional volume of porosity, resulting in a highly fragmented appearance. In Figure 4, the two generations of pores can be clearly distinguished: (i) the 1st generation of pores between the celestine aggregates (yellow star), and (ii) the 2nd generation of pores formed after the transformation of the celestine aggregates into strontianite (pink star).

## Conclusions and Implications

We documented *via* mineralogical and geochemical data sets two rapid and consecutive mineral pseudomorphic replacements taking place through a coupled mechanism of primary phase dissolution-secondary phase crystallisation: i) gypsum single crystals to celestine, and ii) celestine to strontianite. The first transformation occurs upon reaction of gypsum with a Sr solution and proceeds rapidly due to the formation of an extensive network of porosity within the pseudomorph. This porosity compensates the decrease in molar volume between gypsum

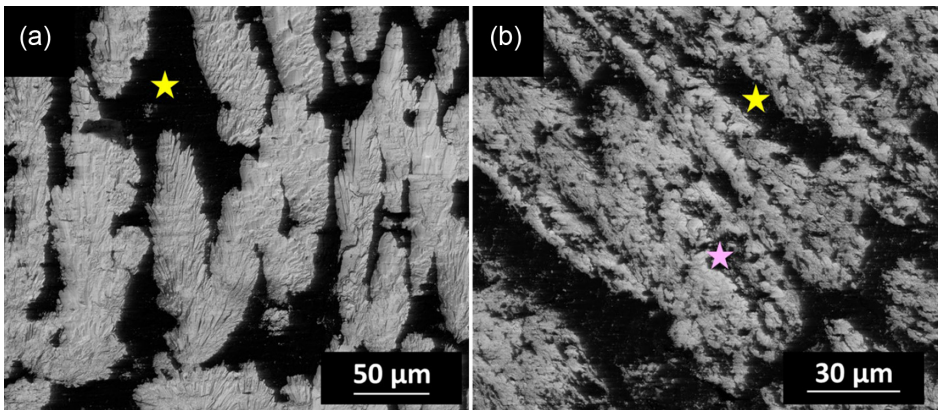


**Figure 4** **(a)** After the transformation of the gypsum single crystals into celestine, the celestine aggregates appear distributed within elongated pores (yellow star). The aggregates appear compact and homogeneous. **(b)** After the transformation of these aggregates into strontianite, the compact aggregates became highly fragmented due to formation of additional porosity (pink star). Both images were obtained in the SEM using BSE.

and celestine. During the second transformation, the celestine pseudomorphs react with a carbonate-rich solution and are replaced by strontianite. The external morphology of the original gypsum precursor remains preserved (again), resulting in strontianite pseudomorphs after gypsum. The preservation of the gypsum morphology occurs because each celestine crystal that formed the first pseudomorph is pseudomorphically replaced itself by smaller crystals of strontianite. Consequently, the outcome of the two replacements are pseudomorphs of strontianite after gypsum, formed by thousands of tiny strontianite pseudomorphs after celestine. During the second transformation, a second generation of porosity within each celestine replaced crystal is formed linked to a further decrease in molar volume.

We have documented, for the first time, that in a double mineral replacement process, the morphology, microtexture and, to some extent the chemistry, of the original precursor can be preserved throughout the whole transformation. As long as dissolution-crystallisation processes are coupled, pseudomorphism can survive successive transformations while retaining textures developed during intermediate transformation stages. These results are crucial for understanding natural mineral replacement phenomena, where the transformations are usually complex and where pseudomorphs can host different mineral phases formed at different stages. Our data provide valuable insights into the significance of pseudomorphs as geological proxies, as this chemical and textural inheritance can be used to reconstruct the geochemical history of the pseudomorph. Furthermore, our data improve our understanding of the complex pseudomorphs found in the geological record. A good example are glendolites, pseudomorphs produced from ikaite ($CaCO_3{\cdot}6H_2O$; *e.g.*, Selleck *et al.*, 2007; Sanchez-Pastor *et al.*, 2016), a carbonate found in cold, polar waters. Ikaite can transform pseudomorphically into calcite, aragonite and/or monohydrocalcite depending on the transformation conditions (Stockmann *et al.*, 2022). Another example is the complex pseudomorphs formed from the weathering of igneous feldspars (Morad *et al.*, 1989). Our results provide useful data for understanding such complex, often consecutive, natural mineral replacement reactions.

## Acknowledgements

This project has received funding from the Helmholtz Recruiting Initiative awarded to LGB (award no. I-044-16-01). JPHP is funded by his independent research fellowship (GFZ Discovery Fund; grant no. P-032-45-002). PF acknowledges support from the PID2021-125467NB-I00 project of the Spanish Ministry of Science, Innovation and Universities. ICP-OES analyses were performed at the Helmholtz Laboratory for the Geochemistry of the Earth Surface at GFZ Potsdam with the assistance of Sebastian Focke. The experiments, XRD, FTIR and SEM analyses were carried out in the laboratories of Environmental Mineralogy and at the Potsdam Imaging and Spectral Analysis (PISA) Facility of section 3.5 (Interface Geochemistry) at the GFZ.

*Editor: Juan Liu*

## Additional Information

**Supplementary Information** accompanies this letter at https://www.geochemicalperspectivesletters.org/article2513.



**Cite this letter as:** Forjanes, P., Perez, J.P.H., Berryman, C., Syczewski, M., Benning, L.G. (2025) Textural and chemical inheritance during a pseudomorphic double mineral transformation. *Geochem. Persp. Let.* 34, 50–56. https://doi.org/10.7185/geochemlet.2513

## References

Altree-Williams, A., Pring, A., Ngothai, Y., Brugger, J. (2015) Textural and compositional complexities resulting from coupled dissolution–reprecipitation reactions in geomaterials. *Earth-Science Reviews* 150, 628–651. https://doi.org/10.1016/j.earscirev.2015.08.013

Beaudoin, N., Hamilton, A., Koehn, D., Shipton, Z.K., Kelka, U. (2018) Reaction-induced porosity fingering: Replacement dynamic and porosity evolution in the KBr-KCl system. *Geochimica et Cosmochimica Acta* 232, 163–180. https://doi.org/10.1016/j.gca.2018.04.026

Centrella, S., Austrheim, H., Putnis, A. (2015) Coupled mass transfer through a fluid phase and volume preservation during the hydration of granulite: An example from the Bergen Arcs, Norway. *Lithos* 236–237, 245–255. https://doi.org/10.1016/j.lithos.2015.09.010

Deer, W.A., Howie, R.A., Zussman, J. (2013) *An Introduction to the Rock-Forming Minerals*. Third Edition, The Mineralogical Society, London. https://doi.org/10.1180/DHZ

Dempster, T., Jess, S.A. (2015) Ikaite pseudomorphs in Neoproterozoic Dalradian slates record Earth's coldest metamorphism. *Journal of the Geological Society* 172, 459–464. https://doi.org/10.1144/jgs2015-018

De Villiers, J.P.R. (1971) Crystal Structures of Aragonite, Strontianite, and Witherite. *American Mineralogist* 56, 758–767. http://www.minsocam.org/ammin/AM56/AM56_758.pdf

Fernández-Díaz, L., Astilleros, J.M., Pina, C.M. (2006) The morphology of calcite crystals grown in a porous medium doped with divalent cations. *Chemical Geology* 225, 314–321. https://doi.org/10.1016/j.chemgeo.2005.08.024

Fernández-Díaz, L., Pina, C.M., Astilleros, J.M., Sánchez-Pastor, N. (2009) The carbonatation of gypsum: Pathways and pseudomorph formation. *American Mineralogist* 94, 1223–1234. https://doi.org/10.2138/am.2009.3194

Forjanes, P., Astilleros, J.M., Fernández-Díaz, L. (2020a) The Formation of Barite and Celestite through the Replacement of Gypsum. *Minerals* 10, 189. https://doi.org/10.3390/min10020189

Forjanes, P., Gómez-Barreiro, J., Morales, J., Astilleros, J.M., Fernández-Díaz, L. (2020b) Epitactic growth of celestite on anhydrite: substrate induced twinning and morphological evolution of aggregates. *CrystEngComm* 22, 5743–5759. https://doi.org/10.1039/D0CE00755B

Howell, R.D., Raju, K., Atkinson, G. (1992) Thermodynamics of "Scale" Mineral Solubilities. 4. Experimental Measurements of $SrSO_4$(s) in $H_2O$ and Aqueous NaCl from 25 to 250 °C and from 1 to 500 bar. *Journal of Chemical & Engineering Data* 37, 464–469. https://doi.org/10.1021/je00008a020

Jonas, L., John, T., King, H.E., Geisler, T., Putnis, A. (2014) The role of grain boundaries and transient porosity in rocks as fluid pathways for reaction front propagation. *Earth and Planetary Science Letters* 386, 64–74. https://doi.org/10.1016/j.epsl.2013.10.050

Leitner, C., Neubauer, F., Marschallinger, R., Genser, J., Bernroider, M. (2013) Origin of deformed halite hopper crystals, pseudomorphic anhydrite cubes and polyhalite in Alpine evaporites (Austria, Germany). *International Journal of Earth Sciences* 102, 813–829. 10.1007/s00531-012-0836-6

Morad, S., Marfil, R., De La Peña, J.A. (1989) Diagenetic K-feldspar pseudomorphs in the Triassic Buntsandstein sandstones of the Iberian Range, Spain. *Sedimentology* 36, 635–650. https://doi.org/10.1111/j.1365-3091.1989.tb02090.x

Nozaka, T., Fryer, P. (2011) Alteration of the Oceanic Lower Crust at a Slow-spreading Axis: Insight from Vein-related Zoned Halos in Olivine Gabbro from Atlantis Massif, Mid-Atlantic Ridge. *Journal of Petrology* 52, 643–664. https://doi.org/10.1093/petrology/egq098

Pina, C.M. (2019) Topotaxial replacement of celestite single crystals by strontianite aggregates: Pseudomorphisation and porosity generation.

*Geochimica et Cosmochimica Acta* 244, 155–162. https://doi.org/10.1016/j.gca.2018.09.032

Pöml, P., Menneken, M., Stephan, T., Niedermeier, D.R.D., Geisler, T., Putnis, A. (2007) Mechanism of hydrothermal alteration of natural self-irradiated and synthetic crystalline titanate-based pyrochlore. *Geochimica et Cosmochimica Acta* 71, 3311–3322. https://doi.org/10.1016/j.gca.2007.03.031

Putnis, A. (2002) Mineral replacement reactions: from macroscopic observations to microscopic mechanisms. *Mineralogical Magazine* 66, 689–708. https://doi.org/10.1180/0026461026650056

Putnis, A. (2009) Mineral Replacement Reactions. *Reviews in Mineralogy and Geochemistry* 70, 87–124. https://doi.org/10.2138/rmg.2009.70.3

Putnis, A. (2015) Transient Porosity Resulting from Fluid–Mineral Interaction and its Consequences. *Reviews in Mineralogy and Geochemistry* 80, 1–23. https://doi.org/10.2138/rmg.2015.80.01

Ruiz-Agudo, E., Putnis, C.V., Putnis, A. (2014) Coupled dissolution and precipitation at mineral–fluid interfaces. *Chemical Geology* 383, 132–146. https://doi.org/10.1016/j.chemgeo.2014.06.007

Sánchez-Pastor, N., Oehlerich, M., Astilleros, J.M., Kaliwoda, M., Mayr, C.C., Fernández-Díaz, L., Schmahl, W.W. (2016) Crystallization of ikaite and its pseudomorphic transformation into calcite: Raman spectroscopy evidence. *Geochimica et Cosmochimica Acta* 175, 271–281. https://doi.org/10.1016/j.gca.2015.12.006

Selleck, B.W., Carr, P.F., Jones, B.G. (2007) A Review and Synthesis of Glendonites (Pseudomorphs after Ikaite) with New Data: Assessing Applicability as Recorders of Ancient Coldwater Conditions. *Journal of Sedimentary Research* 77, 980–991. https://doi.org/10.2110/jsr.2007.087

Shtukenberg, A.G., Punin, Y.O., Gunn, E., Kahr, B. (2012) Spherulites. *Chemical Reviews* 112, 1805–1838. https://doi.org/10.1021/cr200297f

Stockmann, G.J., Seaman, P., Balic-Zunic, T., Peternell, M., Sturkell, E., Liljebladh, B., Gyllencreutz, R. (2022) Mineral Changes to the Tufa Columns of Ikka Fjord, SW Greenland. *Minerals* 12, 1430. https://doi.org/10.3390/min12111430

Xia, F., Brugger, J., Chen, G., Ngothai, Y., O'Neill, B., Putnis, A., Pring, A. (2009) Mechanism and kinetics of pseudomorphic mineral replacement reactions: A case study of the replacement of pentlandite by violarite. *Geochimica et Cosmochimica Acta* 73, 1945–1969. https://doi.org/10.1016/j.gca.2009.01.007

Zhao, J., Brugger, J., Grundler, P.V., Xia, F., Chen, G., Pring, A. (2009) Mechanism and kinetics of a mineral transformation under hydrothermal conditions: Calaverite to metallic gold. *American Mineralogist* 94, 1541–1555. https://doi.org/10.2138/am.2009.3252